Detection of Faults in an Osmotic Dehydration Process Through State Estimation and Interval Analysis

C. A. Collazos[1(✉)], Fredy Sanz[1], I. A. Monroy[2], Adriana Maldonado-Franco[3], Emiro De-la-Hoz-Franco[4], Farid Meléndez-Pertuz[4], and César Mora[5]

[1] Vicerrectoría de Investigaciones, Universidad Manuela Beltrán, Bogotá, D.C, Colombia
cacollazos@gmail.com
[2] Licenciatura en Física, Universidad Distrital, Bogotá, D.C, Colombia
[3] Doctorado en Biociencias, Universidad de la Sabana, Bogotá, D.C, Colombia
[4] Departamento de Ciencias de la Computación y Electrónica, Universidad de la Costa, Barranquilla, Colombia
[5] Centro de Investigación en Ciencia Aplicada y Tecnología Avanzada del Instituto Politécnico Nacional, México DF, Mexico

Abstract. This article shows the results obtained in the application of State Estimation to a case of fault detection and diagnosis in an osmotic dehydration process. The disturbances that affect the measurements on the system are unknown but it is known that they are bounded. The tools used for the development of this work were the EMV (Extended Mean Value) and SIVIA (Set Inversion Via Interval Analysis) algorithms, which allow obtaining the necessary boundaries for the fault detection and diagnosis algorithm. The paper presents simulations and validations.

Keywords: Physics model · Osmotic dehydration · State estimation · Interval analysis · Faults

1 Introduction

Complex systems are subject to stochastic perturbations, which make the process of modeling them difficult to perform. In most cases, the model obtained does not correctly describe the dynamics of the system. Therefore, not having successful models makes it unreliable to carry out a fault detection study and, later, their diagnosis. This paper presents a methodology for state estimation, where the state equations for the process are known and the disturbances are limited through intervals. Interval algebra has diverse applications as shown in [1] and [2].

Currently, Guaranteed State Estimation Methods have been proposed as an alternative to the Stochastic Model Based Estimation, assuming that the disturbances are bounded. This means that the problem is limited to estimating the various states of the system, which makes it is possible to use these results to perform fault detection. State estimation is fundamental for analysis, design, control and supervision of processes in

© Springer Nature Switzerland AG 2019
S. Misra et al. (Eds.): ICCSA 2019, LNCS 11620, pp. 699–712, 2019.
https://doi.org/10.1007/978-3-030-24296-1_56

engineering [3–6]. Specifically, state estimation methodology based on intervals has received a lot of attention in the last few years and literature about this subject shows a growing progress [7–13]. This document presents a review of the existing theory on the technique of guaranteed state estimation, making use of algebra of intervals to implement it in an osmotic dehydration process. The work is structured as follows: Sect. 2 presents the theoretical basis for the guaranteed state estimation and the physical model of the process, on which the technique was applied, Sect. 3 addresses the methodology and the envelope-based fault detection algorithm for each sampling time, Sect. 4 presents the results obtained on the osmotic dehydration process, and finally Sect. 5 collects the conclusions of the work.

2 Theoretical Framework

2.1 Problem Statement

The unknown state x for a dynamic system is defined by:

$$\dot{x}(t) = f(x(t)), y(t) = g(x(t)),\ x(0) \in [X_0] \tag{1}$$

where $x(t) \in R^n$ and $y(t) \in R^n$, and they denote, respectively, the state variables and the outputs of the system. Initial conditions $x(0)$ are supposed to belong to an initial "box" $[X_0]$. The concept of "box" will be described in Sect. 3. Time is $t \in [0, t_{max}]$. The functions f and g are real and can be differentiable in M, where M is an open set of Rn, such as $x(t) \in$ M for each $t \in [0, t_{max}]$. Besides, function f is at least k-times differentiable in the M domain. The output error is defined by:

$$v(t_i) = y(t_i) - y_m(t_i), i = 1, 2, \ldots, N. \tag{2}$$

We assume that $\underline{v(t)}$ and $\overline{v(t)}$ represent the lower and upper limit of acceptable output error, respectively. These limits correspond to a bounded noise. The integer number N is the total number of records. The interval arithmetic are used to calculate the guaranteed limits for the solution of Eq. 1 in the sampling times $\{t_1, t_2, \ldots, t_N\}$. Even though the studied process is a continuous dynamic system, Eq. 2 indicates that the problem statement is applicable for a discrete system, which is governed by difference equations [4].

2.2 Studied Process (Osmotic Dehydration of Pineapple)

The osmotic dehydration process has highly complex dynamics, which implies that there are a great variety of models and experimental procedures for different kinds of fruits and foods [14–16] and [17]. Independent of the chosen model, some authors coincide that the most significant variables of the process are identified with the food concentration and the concentration of the solution where the food is immersed in [18] and [19]. Pineapple is a completely heterogeneous, highly watery and porous food, that when immersed in solutions with high concentration of soluble solids (sugar), provokes

two simultaneous upstream main flows. The first flow corresponds to a transfer of soluble solids (sugar) from the solution to the food. The second one is flow of water from the food that goes highly concentrated to the solution. A third secondary and negligible flow of aroma, vitamins and minerals happens, which is less intense, and occurs from the fruit to the solution. The mass transfer mechanisms that are present in the osmotic dehydration at atmosferic pressure and room temperature are mainly diffusion (Fick's laws of diffusion). These mechanisms are originated by the concentration differences between the food and the osmotic solution where the fruit is immersed in [18, 19] and [20]. Figure 1 shows the previously described flows that occur during the osmotic dehydration.

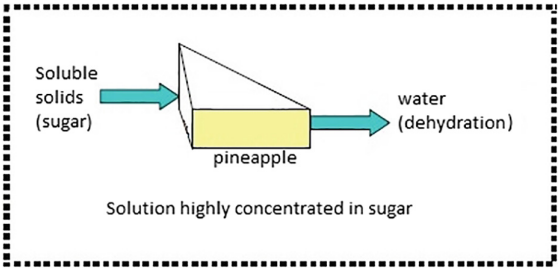

Fig. 1. Mass transfer process between solution and fruit

The sugar concentrations found in the osmotic solution and the fruit are registered by refractometers and reported in refraction indexes or Degrees Brix.

Degrees Brix can be understood as a percentage from 0 to 1 or a mass fraction, that provides the sugar mass contained in the mass of each analyzed component (solution and fruit). The model that was studied in this paper was extracted from [18] and it considers three state variables: concentration in fruit, concentration in tank 1 solution and volume that enters tank 1 from tank 2. The dehydration plant and its operation is described in [18, 19] and [20]. Figure 2 shows the process.

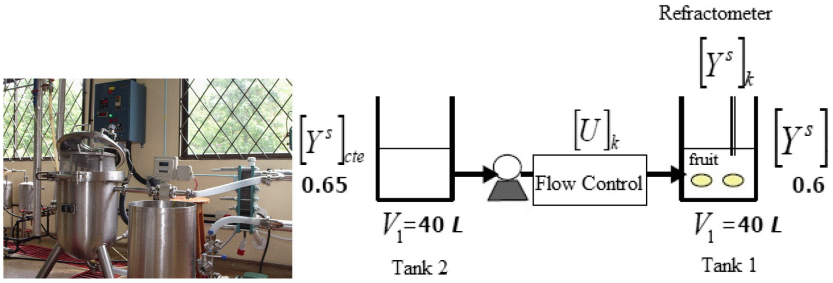

Fig. 2. Pineapple osmotic dehydration process diagram, (Unitary Operations Laboratory - Unisabana)

The model of [18] assumes that there is a perfect mix in tank 1, where the flow is perfectly controlled and the values for concentration in fruit and in tank 1 obey ideally to mass balances. The process is modeled in a discrete manner with a sample time of ΔT. The model is represented by difference equations, as indicated below:

Variation of Sugar Concentration for the Solution:

$$[Y^s]_{k+1} = [Y^s]_k - B[C]_k[X^s]_k\Delta T + ([Y^s]_{cte} - [Y^s]_k)[U]_k\Delta T/[V]_k \tag{3}$$

Variation of Sugar Concentration for the Food:

$$[X^s]_{k+1} = [X^s]_k + [C]_k[X^s]_k\Delta T + [U]_k[X^s]_k\Delta T/[V]_k \tag{4}$$

Where:

$[V]_k$ is the variation of thank 1 volume:

$$[V]_{k+1} = [V]_k + [U]_k\Delta T \tag{5}$$

$[C]_k$ is the variation of thank 1 volume:

$$[C]_k = \mu\frac{[Y^s]_k}{K_{Y^s} + [Y^s]_k} \tag{6}$$

B is a dimensionless proportion factor between the concentration variation of the solution and that of the food. This parameter is calculated using the final (subindex f) and initial (subindex o) values of the concentrations in solution and food during an experimental process:

$$B = \frac{[Y^s]_f - [Y^s]_o}{[X^s]_f - [X^s]_o} \tag{7}$$

μ is the maximum change rate in sugar growth for the food. It is represented by:

$$\mu = \frac{ln\left(\frac{[Y^s]_f}{[X^s]_o}\right)}{(t_f - t_i)} \tag{8}$$

$\boldsymbol{K_{Y^s}}$ = 0.65 (gr. of sugar/gr. of osmotic solution in tank (1) is the saturation constant for sugar concentration in tank 1. The raw material associated to the presented model is pineapple (*ananas comosus* in the cayena lisa variety) in a geometric shape (eighths of slice of 1 cm of thickness without any previous treatment).

The attributes of the osmotic solution for each tank were:

Tank 2: Constant. $\left[\boldsymbol{Y^S}\right]_{\boldsymbol{cte}}$ = 0.65° Brix.

Tank 1: Reference. $\left[\boldsymbol{Y^S}\right]_{\boldsymbol{ref}}$ = 0.6° Brix.

The process was simulated for a constant lineal entry flow: $[U2]_k$: (0 to 2.09) L/min for 180 min. The calculation of the kinetic parameter $[C]_k$ and the kinetic constants μ = 0.0007 L/min and $B = 0.27$ are assumed as known.

3 Methodology

3.1 Interval Analysis Fundamentals

At first, interval analysis was a response to explain quantification errors that occurred when real numbers were represented rationally in computers and the technique was extended to validated numerics [30]. According to [30], an interval [u] = [$\underline{u}$, $\bar{u}$], is a closed and connected subset of R, denoted by $\boldsymbol{IR}$. Two intervals $[u]$ and $[v]$ are equal, if and only if their inferior and superior limits are the same. Arithmetic operations between two intervals $[u]$ and $[v]$, can be defined by:

$$o \in \{+, -, *, \div\}, [u]o[v] = \{xoy / [u], y \in [v]\} \tag{9}$$

The interval vector (or box) $[X]$ is a vector with interval components and it is equivalent to the cartesian product of scalar intervals:

$$[X] = [x_1] \times [x_2] \ldots \times [x_n]. \tag{10}$$

The vector set of real n-dimensional intervals is denoted by $\boldsymbol{IR}^n$. A matrix interval is a matrix where its components are intervals. The set of $n \times m$ real interval matrices is denoted by $\boldsymbol{IR}^{n*m}$. The classic operations for interval vectors or interval matrices are direct extensions of the same operations of point vectors [30].

The operations for punctual vectors can be extended to become classical operations for interval vectors [22]. This way, if: $\boldsymbol{f} : R^n \rightarrow R^m$, the range of function f in an interval vector $[u]$, is given by:

$$f([u]) = \{f(x) / x \in [u]\} \tag{11}$$

The interval function $[f]$ of $\boldsymbol{IR}^n$ to $\boldsymbol{IR}^m$ is a function of the inclusion of f if:

$$\forall [u] \in \boldsymbol{IR}^n, f([u]) \subseteq [f]([u]) \tag{12}$$

An inclusion function of f can be obtained through the substitution of each occurrence of a real variable for its corresponding interval. Said function is called natural inclusion function. In practice, the inclusion function is not unique, and it depends on the syntax of f [30].

3.2 Inversion Set

Consider the problem of determining a solution set for the unknowns u, defined by:

$$S = \{u \in U / \Phi(u) \in [y]\} = \Phi^{-1}([y]) \cap U \tag{13}$$

where $[y]$ is known a priori, U is a search set for u and Φ of an invertible nonlinear function, which is not necessarily in the classical sense. [9] includes the calculation of the reciprocal image of Φ and that is known as a set inversion problem that can be solved using the SIVIA (Set Inversion Via Interval Analysis) algorithm. SIVIA as proposed in [9] is a recursive algorithm that goes through all the searching space so it does not lose any solution. This algorithm makes it possible to derive a guaranteed enclosure of the solution of set S, that meets: S is factible, enough to prove that $\Phi([u]) \subseteq [y]$. Conversely, if it can be proven that $\Phi([u]) \bigcap [y] = 0$, then the box $[u]$ is non-viable. On the contrary, there is no conclusion and the box $[u]$ is said to be undetermined. If the box is undetermined, the box is bisected and tried again until its size reaches a threshold precision, specified for $\varepsilon > 0$. This criterion assures that SIVIA finishes after a limited number of iterations.

3.3 State Estimation

State estimation refers to the integration of Eq. 1. Thus, the goal is to estimate the state of vector $\boldsymbol{x}$ in the sampling times $\{t_1, t_2, \ldots, t_N\}$, which correspond to the times of output measurements. The box $\left[x\left(t_j\right)\right]$ is denoted as $[x_j]$, where t_j represents the sampling time, j = 1, 2, …, N and x_j represents the solution of 1 at t_j. For models like the one presented in 1, the sets are characterized by not being convex and there could even be several disconnected components. Interval analysis consists of enclosing said sets in interval vectors that do not overlap and the usual inconvenient is obtaining wider solution interval vectors each time. This in known as the Wrapping Effect. This way, the wrapping effect yields poor results. The poverty brought by the big width of the set can be reduced through the use of a higher-order k for the Taylor expansion and through the use of mean value forms and matrices of pre-conditioning [13] and [23].

3.4 Prediction and Correction

Prediction aims at calculating the accessibility fixed for the state vector, while the correction stage keeps only the parts of the accessibility set that are consistent with the measurements and the error limits defined by Eq. 2. It is assumed that $\left[X_j\right]$ is a box that is guaranteed to contain x_j at t_j. The exterior aproximation of the predicted set $[X_{j+1}^{+}]$ is defined as the validated solution of the difference equation at t_{j+1}. The set $\left[X_{j+1}^{+}\right]$. is calculated using the EMV algorithm (extenden mean value), defined in [23]. The set is guaranteed to contain the state at t_{j+1}. At t_{j+1}, a "measurement vector", $[y_{j+1}]$, is obtained and it corresponds to the upper and lower limits for measurement noise.

$$[y_{j+1}] = \left[y_{j+1} - \underline{v_{j+1}}, -\overline{v_{j+1}}\right] \tag{14}$$

Then, the set $[g]^{-1}([y_{j+1}])$. is calculated. This evaluation is obtained by the SIVIA algorithm. The expected solution at the sampling time t_{j+1} is finally given by $[x_{j+1}] = \left[X_{j+1}^{+}\right] \bigcap [g]^{-1}([y_{j+1}])$. The procedure for the state estimation is summarized in the following algorithm: For $j = 0$ to $j = N - 1$ do:

Prediction step: compute $[X_{j+1}^{+}]$ using EMV algorithm.

Correction step: calculate $[x_{j+1}]$ so that

$$[x_{j+1}] = \left[X_{j+1}^{+}\right] \bigcap [g]^{-1}([y_{j+1}]),$$

3.5 Extended Mean Value (EMV)

The most efficient methods to solve state estimation for dynamic systems are based on Taylor's expansions [23]. These methods consist of two parts: the first part verifies the existence and uniqueness of the solution, using the fixed point theorem and the Picard-Lindelf operator. At a time t_{j+1}, a box, a priori $[\tilde{x}_j]$, that contains all the solutions that correspond to all the possible trajectories between tj and t_{j+1} is obtained. In the second part, the solution at t_{j+1} is calculated using Taylor's expansion, in the term that remains is $[\tilde{x}_j]$. However, in practice, the set $[\tilde{x}_j]$ often doesn't contain the true solution [24]. Therefore, the used technique consists of inflating this set until the next inclusion is verified with the following expression:

$$[x_j] + hf([\tilde{x}_j]) \subseteq [\tilde{x}_j] \tag{15}$$

where h indicates the integration stage and $[X_j]$ is the first solution. This method is summarized in the Enclosure algorithm, which was developed by [25]. The inputs are $[x_j]$ and $\alpha > 0$ and the output is $[\tilde{x}_j]$:

$$[x_j] = [\tilde{x}_j]$$

$$\text{While } ([x_j] + hf([\tilde{x}_j]) \sim \subseteq [\tilde{x}_j] \text{ do :}$$

$$[\tilde{x}_j] = inflate([\tilde{x}_j], \alpha).$$

The function inflate for an interval vector $[u] = \left[\underline{u_1}, \overline{u_1}\right], \ldots, \left[\underline{u_n}, \overline{u_n}\right]$, operates as follows:

$$\left[(1-\alpha)\underline{u_1}, (1+\alpha)\overline{u_1}\right], \ldots, \left(\left[(1-\alpha)\underline{u_n}, (1+\alpha)\overline{u_n}\right]\right).$$

Precision depends of the α coefficient. If the set $[\tilde{x}_j]$ satisfies the inclusion presented in Eq. 15, then the inclusion $x(t) \in [\tilde{x}_j]$ is maintained for all $t \in [t_j, t_{j+1}]$. The solution

x_{j+1} of the differential equation given in Eq. 1 at t_{j+1} is guaranteed, in the interval vector $[x_{j+1}]$ and it is given by the Taylor expansion [30]:

$$[x_{j+1}] = [x_j] + \sum_{i=1}^{k-1} h^i f^{[i]}([x_j]) + h^k f^{[k]}([\tilde{x}_j]), \tag{16}$$

where $\boldsymbol{k}$ denotes the end of the Taylor expansion and the $f^{[i]}$ coefficients are the Taylor coefficients of the $\boldsymbol{x}(\boldsymbol{t})$ solution, which are obtained in a recursive form by:

$$f^{[1]} = f, f^{[i]} = \frac{1}{i}\frac{\partial f^{[i-1]}}{\partial x} f, i \geq 2 \tag{17}$$

The application of the inflate function in the set $[\tilde{x}_j]$ leads to increase of its width. The poor quality introduced by the wider set can be reduced through the use of a higher order $\boldsymbol{k}$ for the Taylor expansion in Eq. 17. But the width of the solution always increases, even for higher orders. To sort this obstacle, Rihm [26] proposes evaluating 17 through the extended mean value algorithm, based on mean value forms and pre-conditioning matrices. This algorithm is used to solve the differential equation given in 1. The inputs for this algorithm are $[\tilde{x}_j], [x_j], \hat{x}_j, [v_j], p_j, A_j, h$ and the outputs are $[\widetilde{x_{j+1}}], \hat{x}_{j+1}, [v_{j+1}], [p_{j+1}], A_{j+1}$. The variable $\hat{x}_j$ is the mean point of a certain interval v_j. The initial conditions may be provided by $p_0 = 0, q_0 = 0$ and $v_0 = x_0$. Up next, the secuence of the algorithm is presented:

a. $[v_{j+1}] = \hat{x}_j + \sum_{i=1}^{k-1} h^i f^{[i]}(\hat{x}_j) + h^k f^{[k]}([\tilde{x}_j])$,
b. $[S_j] = I + \sum_{i=1}^{k-1} J(f^{[i]}; [x_j]) h^i$,
c. $[q_{j+1}] = ([S_j]A_j)[P_j] + [S_j]([v_j]) - \hat{x}_j)$,
d. $[x_{j+1}] = [v_{j+1}] + [x_{j+1}]$
e. $A_{j+1} = m([S_j]A_j)$,
f. $p_{j+1}] = A_{j+1}^{-1}([S_j]A_j)[p_j] + \left(A_{j+1}^{-1}[S_j]\right)([v_j] - \hat{x}_j)$,
g. $\hat{x}_{j+1} = m([v_{j+1}])$

In the previous algorithm, I represents the identity matrix (with the same dimension of the state vector). $J(f^{[i]}; [x_j])$ is the Jacobian matrix of the Taylor coefficient, $f^{[i]}$, which is evaluated over $[x_j]$. The variables $\hat{x}_j$ and $[v_j]$ are calculated in the state $(t_j - 1)$.

3.6 Envelope-Based Fault Detection and Diagnosis Algorithm

The detection of a fault, in practice, is a difficult task to perform due to the imprecision presented by the mathematical models that are available for a given process. Generally, a failure is detected when the measured value Y_M does not correspond to the reference value, Y_R, which is provided by the model, as indicated by the Eq. 18.

$$Y_M \bigcap Y_R = 0 \tag{18}$$

When having interval models of the process, it is feasible to estimate its state, considering the variations of its parameters and the perturbations obtained due the presence of noise in the measurement. This allows determining if a system is:

a. Functioning normally

b. Has a fault that has not been detected, or a false alarm was generated

c. Failing

The envelope-based fault detection algorithm proposes the assignment of three regions:

a. The external region, which corresponds to values that are outside the interval limits of the worst case evaluated for the system, where it has a particularly large amount of noise.

b. The intermediate region, which corresponds to values that are between the worst case and the best case evaluated.

c. The internal region, which corresponds to values that are located within the interval range of the best case, where it displays little presence of noise and a smaller interval width than the worst case.

To determine the envelopes and assign the three regions, the state estimation for nonlinear systems presented in the previous section is used. Once the regions have been determined, we proceed with the evaluation of the type of system operation (Normal, Failure not detected or measurement error, Failed).

The fault detection algorithm is shown below:

h. *Inputs* : Y_M, R_S, W_S.

i. *Outputs* : $[Faults]$

j. *If* $[Y_M > Up_W_S] \vee [Y_M < Low_W_S]$

k. *then Fault* (-1)

l. *If* $[Y_M < Up_W_S]^{\wedge}[Y_M > Up_B_S]$

m. *Then Fault* that has not been detected, or a false alarm (1)

n. *If* $[Y_M > Low_W_S]^{\wedge}[Y_M < low_B_S]$

o. *Then Fault* that has not been detected, or a false alarm (1)

p. *If* $[Y_M < Up_B_S]^{\wedge}[Y_M > low_B_S]$

q. *Then Normal* (0)

Where:

Y_M: It is the measured response of the system.

B_S: It is the envelope for the best case scenario.

W_S: It is the envelope for the worst case scenario.

4 Results and Analysis

The state estimation algorithm is applied to the pineapple dehydration model. The analysis is taken to simulation level. Noise R is delimited for the state $[Y^s]$, $[X^s]$ and $[V]$ respectively, as follows:

$$R = \begin{bmatrix} -0.05 & 0.05 \\ -0.05 & 0.05 \\ -0.05 & 0.05 \end{bmatrix} \tag{18}$$

The initial conditions for the state variables $[Y^s], [X^s]$ and $[V]$, are given by:

$$x(0) = \begin{bmatrix} 0.135 & 0.145 \\ 0.600 & 0.610 \\ 40.45 & 40.55 \end{bmatrix} \tag{19}$$

Figures 3, 4 and 5 show the prediction envelope, starting with the estimation envelope (lower and upper EMV), then determining the solution set of the state by means of (lower and upper SIVIA). This way, we obtain the two envelopes that guarantee the status for each sampling time, in each of the output variables. The reference concentration of the process under normal conditions corresponded to 0.65 degrees brix for tank 1 and the data are shown in solid black line for each of the state variables.

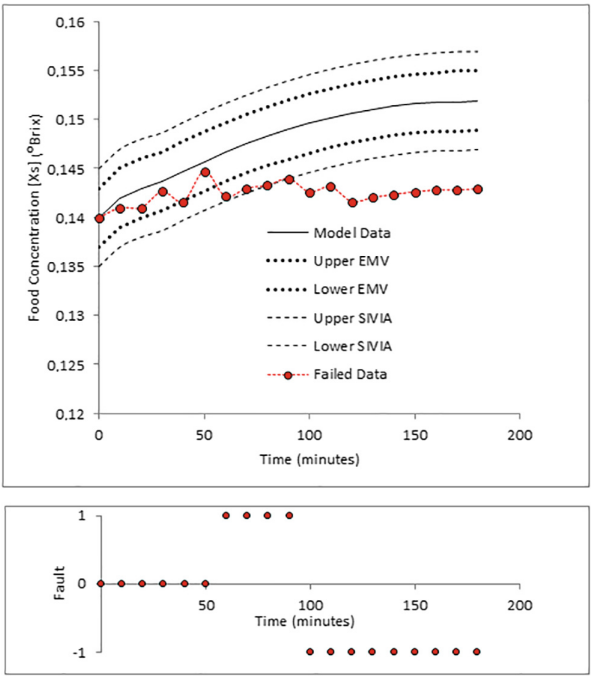

Fig. 3. Resulting envelope from state and failure estimation for food concentration

Figures 3, 4 and 5 also indicate the results obtained for the detection of faults on the system, which correspond to the presence of an inflow of less than $[U2]_k$: (0 to 1.09) L/min with a sampling time of 10 min. This modifies the response of the system in

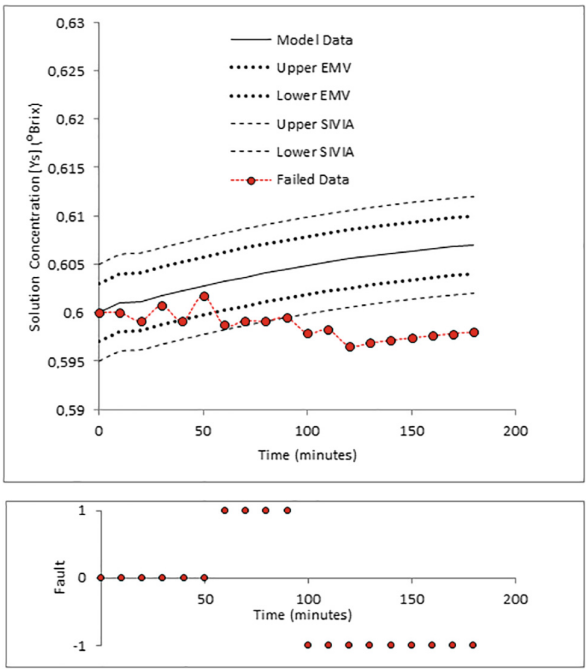

Fig. 4. Resulting envelope for state and failure for solution concentration.

each of the state variables compared to the reference model. The data of the output variables for the new input are shown in continuous red line. The reference concentration for the new input was 0.6° brix for tank 1. The diagnosis of the faults is indicated in the lower part of each of the graphs under the following convention:

(−1): System Failure

(1): The system presents an undetected failure or a false alarm is present, which may be triggered by measurement noise.

(0): System is functioning correctly

Figures 3, 4 and 5 show the response of the system under normal operating conditions, in a time interval of 0 to 50 min. It is shown how the alarm signal (1) is maintained when the system output is located between the interval corresponding to [EMV-lower, SIVIA lower], in a time interval between 60 and 90 min. A failure occurs at t = 100 min, which is shown as the food concentration, solution concentration and food concentration rate begin to decrease at this moment and keep this trend.

From the previous graphs, it can be seen how the envelopes generated by the estimation of states allow to evaluate the behavior of a system and thus determine whether or not it has faults. The purpose of this proposed solution is to perform efficient monitoring of the output of a system at a low computational cost and considering the measurement variability as a result of the disturbances.

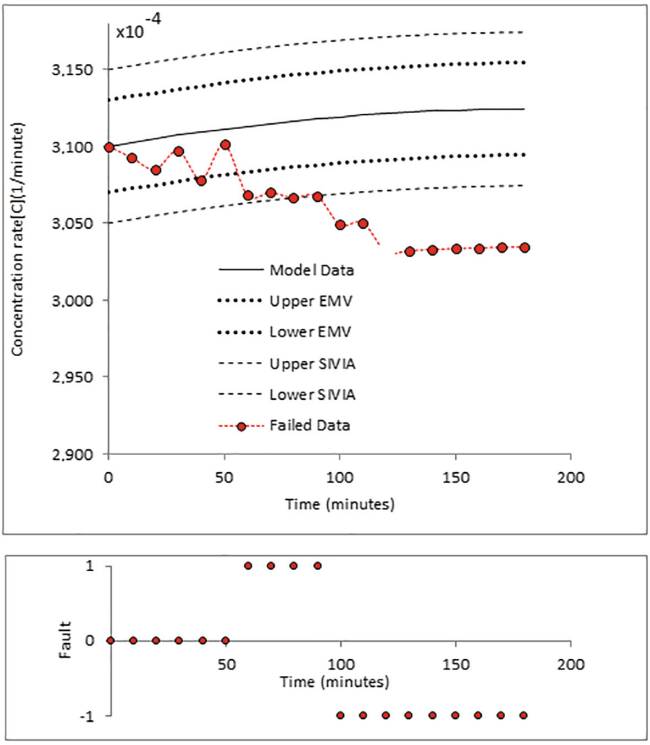

Fig. 5. Resulting envelope for state and failure estimation for food concentration rate.

5 Conclusions

When implementing and applying the estimation technique by the EMV algorithm, it was found that this guarantees the inclusion of the real state within the obtained prediction, as well as the decrease of the wrapping effect, since it makes use of the concept of midpoint interval to calculate an optimal estimate.

The SIVIA algorithm yielded a solution set coherent to the response of the system, which is based on the process model, meaning that the model adequately represents the dynamics of the system. Using the regions for the detection and diagnosis of faults, it is feasible to determine reliable intervals for the correct functioning of the system.

Likewise, the precision of the regions is directly related to the level of uncertainty that is considered for the generation of the envelopes, which varies from process to process and depends on the accuracy of the taken measurements.

By using the classic prediction-correction scheme through the use of the EMV and SIVIA algorithms, it is possible to propose ON-LINE detection and diagnosis techniques given the low computational cost involved in these methods.

As future work, existing control techniques applied in intervals can be used, which allow to control processes within ranges, which contrasts with the classic techniques of automatic control.

The methodology used in this work is applicable to real processes such as those shown in [28, 29] and [30] and may be used for failure detection and diagnostics.

References

1. Burgos, M., González, A., Vallejo, M., Izquierdo, C.: Selección económica de equipo utilizando matemáticas de intervalos. Información Tecnológica **9**(5), 311–316 (1998)
2. Campos, P., Valdés, H.: Optimización Global por Intervalos: Aplicación a Problemas con Parámetros Inciertos. Información Tecnológica **17**(5), 67–74 (2006)
3. Zapata, G., Cardillo, J., Chacón, E.: Aportes Metodológicos para el Diseño de Sistemas de Supervisión de Procesos Continuos. Información tecnológica **22**(3), 97–114 (2011)
4. Jauberthie, C. and Chanthery, E., Optimal input design for a nonlinear dynamical uncertain aerospace system. In: IFAC Symposium on Nonlinear Control Systems, Toulouse-France (2013)
5. Li, Q., Jauberthie, C., Denis, L., Cher, Z.: Guaranteed State and Parameter Estimation for Nonlinear Dynamical Aerospace Models, Informatics in Control, Automation and Robotics (ICINCO), Vienna, Austria (2014)
6. Ortega, F., Pérez, O., López, E.: Comparación del desempeño de estimadores de estado no lineales para determinar la concentración de biomasa y sustrato en un bioproceso. Información tecnológica **26**(5), 35–44 (2015)
7. Kieffer, M., Jaulin, L., Walter, E.: Guaranteed recursive nonlinear state bounding using interval analysis. Int. J. Adaptative Control Sig. Process. **16**(3), 193–218 (2002)
8. Jaulin, L.: A nonlinear set membership approach for the localization and map building of underwater robots. IEEE Trans. Rob. **25**(1), 88–98 (2009)
9. Jaulin, L., Walter, E.: Set inversion via interval analysis for nonlinear bounded-error estimation. Automatica **29**(4), 1053–1064 (1993)
10. Paşca, I.: Formally verified conditions for regularity of interval matrices. In: 10th International Conference, AISC 2010, 17th Symposium, Calculemus 2010, and 9th International Conference, MKM 2010, Paris- France (2010)
11. Rauh, A., Auer, E.: Modeling, Design and Simulation of Systems with Uncertaintites. Springer, Berlin (2011). https://doi.org/10.1007/978-3-642-15956-
12. Jauberthie, C., Verdiere, N., Trave, L.: Fault detection and identification relying on set-membership identifiability. Ann. Rev. Control **37**(1), 129–136 (2013)
13. Nedialkov, N.: Vnode-lp a validated solver for initial value problems in ordinary differential equations. Technical report, Department of Computing and Software (2006)
14. Arreola, S., Rosas, M.: Aplicación de vacío en la deshidratación osmótica de higos (ficus carica). Información tecnológica **18**(2), 43–48 (2007)
15. Arballo, J.: Modelado y simulación de la deshidratación combinada osmótica de frutihortícolas. Ph.D. Thesis in Engineering, Universidad de La Plata, Argentina (2013)
16. García, A. y otros cuatros autores, Análisis comparativo de la cinética de deshidratación Osmótica y por Flujo de Aire Caliente de la Piña (Ananas Comosus, variedad Cayena lisa). Rev Cie Téc Agr **22**(1), 62–69 (2013)
17. García, M., Alvis, A., García, C.: Evaluación de los pretratamientos de deshidratación osmótica y microondas en la obtención de hojuelas de mango (Tommy Atkins). Información tecnológica **26**(5), 63–70 (2015)

18. Jaller, S., Vargas, S.: Comparación de la Transferencia de materia en los procesos de Deshidratación Osmótica a presión atmosférica y con impregnación de vacío en la piña cayena lisa (ananás comosus l. meer) a través de un modelo matemático, Tesis de Pregrado en Ingeniería de Producción Agroindustrial, UniSabana, Chía, Colombia (2000)
19. Gonzalez, G.: Viabilidad de la Piña colombiana var. Cayena Lisa, para su industrialización combinando las operaciones de Impregnación a vacío, deshidratación cayena lisa (ananás comosus meer), Tesis de Doctorado, Universidad Politécnica de Valencia, Valencia, España (2000)
20. Wullner, B.: Instrumentación y Control de un deshidratador Osmótico a Vacío, Tesis de Pregrado en Ingeniería de Producción Agroindustrial, UniSabana, Chía, Colombia (1998)
21. Moore, R.: Automatic error analysis in digital computation, Technical report LMSD-48421, Lockheed Missiles and Space Co, Palo Alto, CA (1959)
22. Moore, R.E.: Interval Analysis. Prentice Hall, New Jersey (1966)
23. Nedialkov, N., Jackson, K., Pryce, J.: An effective high-order interval method for validating existence and uniqueness of the solution of an IVP for an ode. Reliable Comput. **7**, 449–465 (2001)
24. Milanese, M., Norton, J., Piet-Lahanier, H., Walter, W.: Bounding Approaches to System Identification. Springer, Boston (1996). https://doi.org/10.1007/978-1-4757-9545-5
25. Lohner, R.: Enclosing the Solutions of Ordinary Initial and Boundary Value Problems, pp. 255–286. Wiley-Teubner, Stuttgart (1987)
26. Rihm, R.: Interval methods for initial value problems in ODEs. In: Herzberger, J. (ed.) Topics in Validated Computations: Proceedings of the IMACS-GAMM International Workshop on Validated Computations, University of Oldenburg, Elsevier Studies in Computational Mathematics. Elsevier, Amsterdam (1994)
27. Walter, É., Pronzato, L.: Identification de mod`eles parametriques à partir de donnees experimentales. Masson (1994)
28. Castellanos, H.E., Collazos, C.A., Farfán, J.C., Meléndez-Pertuz, F.: Diseño y Construcción de un Canal Hidráulico de Pendiente Variable. Información tecnológica **28**(6), 103–114 (2017). https://dx.doi.org/10.4067/S0718-07642017000600012. Accessed 20 July 2018
29. Collazos, C.A., Castellanos, H.E., Burbano, A.M., Cardona, J.A., Cuervo, J.A., Maldonado-Franco, A.: Semi-mechanistic modelling of an osmotic dehydration process. WSEAS Trans. Syst. **16**, 27–35 (2017). E-ISSN: 2224-2678, Bulgary
30. Duarte, J., Garcia, J., Jimenez, J., Sanjuan, M.E., Bula, A., Gonzalez, J.: Autoignition control in spark-ignition engines using internal model control structure. J. Energy Resour. Technol. **139**(2), 022201 (2016)